

The quantum sweeper effect

G Grössing, S Fussy, J Mesa Pascasio and H Schwabl

Austrian Institute for Nonlinear Studies, Akademiehof, Friedrichstr. 10, 1010 Vienna, Austria

E-mail: ains@chello.at

Abstract. We show that during stochastic beam attenuation in double slit experiments, there appear unexpected new effects for transmission factors below $a \lesssim 10^{-4}$, which can eventually be observed with the aid of weak measurement techniques. These are denoted as *quantum sweeper* effects, which are characterized by the bunching together of low counting rate particles within very narrow spatial domains. We employ a “superclassical” modeling procedure which we have previously shown to produce predictions identical with those of standard quantum theory. Thus it is demonstrated that in reaching down to ever weaker channel intensities, the nonlinear nature of the probability density currents becomes ever more important. We finally show that the resulting unexpected effects nevertheless implicitly also exist in standard quantum mechanics.

1. Introduction

In his criticism of David Bohm’s causal interpretation of the quantum mechanical formalism, Isidor Rabi made the following statement in the 1950ies which is still shared by quite some researchers today: “I do not see how the causal interpretation gives us any line to work on other than the use of the concepts of quantum theory. Every time a concept of quantum theory comes along, you can say yes, it would do the same thing as this in the causal interpretation. But I would like to see a situation where the thing turns around, when you predict something and we say, yes, the quantum theory can do it too.” [1]

Although doubtlessly the project of a causal interpretation à la de Broglie–Bohm has gained momentum in recent years, with many of its results exhibiting more detailed illustrations via particle trajectories, in fact no experimental prediction unknown to orthodox quantum theory has yet arisen from this approach.

However, in the present paper we discuss a finding based on a causal view of quantum mechanics that amounts to a new effect which has so far eluded orthodox quantum mechanics. Specifically, we recently reported theoretical results from extreme beam attenuation techniques in double-slit experiments whose phenomenology is described by what we term the *quantum sweeper effect*. [2] The discovery of this effect is due to our causal subquantum model for quantum systems, whose central features can be shown to exactly match with the de Broglie–Bohm theory [3].

In Chapter 2 of this paper, we firstly present the quantum sweeper effect in said subquantum scenario. Chapter 3, then, discusses the consequences of the mentioned beam attenuation techniques in purely quantum mechanical language, thus showing that the latter does provide statements in line with, but not as detailed as, the effect described in subquantum terms.

Finally, in Chapter 4 we shall discuss the significance of the sweeper effect. Essentially, we show that in employing ever weaker channel intensities, nonlinear effects become ever more



important, which are generally not considered – although implicitly present – in ordinary quantum mechanics. The latter are a crucial characteristic of subquantum models as the one developed by our group, with experimental tests becoming feasible through the use of weak measurement techniques. Consequences are also discussed with respect to the meaning of the complementarity principle in the light of our new findings.

Before we discuss the sweeper effect, however, some preliminaries are necessary in order to provide the appropriate context. To begin with, we recall from [4, 5] that a beam chopper was employed as a deterministic absorber in one arm of a two-armed interferometer, whereas for stochastic absorption semitransparent foils of various materials were used. Despite the net effect of the same percentage of neutrons being attenuated, the quantum mechanical formalism predicts the following different behaviors for the two cases. Introducing the *transmission factor* a as the beam’s transmission probability, in the case of a (deterministic) chopper wheel it is given by the temporal open-to-closed ratio, $a = \frac{t_{\text{open}}}{t_{\text{open}} + t_{\text{closed}}}$, whereas for a (stochastic) semitransparent material defined by its absorption cross section, it is simply the relation of the intensity I with absorption compared to the intensity I_0 without, i.e. $a = I/I_0$. Thus the beam modulation behind the interferometer is obtained in the following two forms. For the deterministic chopper system the intensity is, with φ denoting the phase difference, given by

$$I \propto (1 - a) |\Psi_1|^2 + a |\Psi_1 + \Psi_2|^2 \propto 1 + a + 2a \cos \varphi, \quad (1)$$

whereas for stochastic beam attenuation with the semitransparent material it is

$$I \propto |\Psi_1 + \Psi_2|^2 \propto 1 + a + 2\sqrt{a} \cos \varphi. \quad (2)$$

In other words, although the same number of neutrons is observed in both cases, in the first one the contrast of the interference pattern is proportional to a , whereas in the second case it is proportional to \sqrt{a} .

In [2] we accounted for the just described attenuation effects, and we chose the usual double slit scenario, primarily because this turned out to be very useful when discussing more extreme intensity hybrids (i.e., combinations of high and very low transmission factors). Moreover, in this way we could make simple use of the essentials of our model which are employed in our explanation of the beam attenuation phenomena.

Throughout the last years we have developed an approach to quantum mechanics within the scope of theories on “Emergent Quantum Mechanics”. (For the proceedings of the first two international conferences devoted to this subject, see [6, 7].) Essentially, we consider the quantum as a complex dynamical phenomenon, rather than as representing some ultimate-level phenomenon in terms of, e.g., pure formalism, wave mechanics, or strictly particle physics only. Our assumption is that a particle of energy $E = \hbar\omega$ is actually an oscillator of angular frequency ω phase-locked with the zero-point oscillations of the surrounding environment, the latter of which containing both regular undulatory and fluctuating components and being constrained by the boundary conditions of the experimental setup via the emergence of standing waves. In other words, the particle in this approach is an off-equilibrium steady-state maintained by the throughput of zero-point energy from its vacuum surroundings. This is in close analogy to the bouncing/walking droplets in the experiments of Couder and Fort’s group [8–10], which in many respects can serve as a classical prototype guiding our intuition. However, we denote our whole ansatz as “superclassical” [7], because it connects the classical physics at vastly different scales, i.e. the ordinary classical one and an assumed subquantum one, with “new” effects emergent on intermediate scales, which we have come to know and describe as quantum ones.

In fact, we have succeeded in reproducing a number of quantum mechanical results with our superclassical model, i.e. without any use of the quantum mechanical formalism, like states, wave functions, *et cetera*. Note, moreover, that a Gaussian emerging from, say, a single slit

with rounded edges (so as to avoid diffraction effects) is in our model the result of statistically collecting the effects of the aleatory bouncing of our particle oscillator. Rather, the Gaussian stands for the statistical mean of the “excitation” (or “heating up”) of the medium within the confines of the slit, and later, as the bouncer/walker progresses, further away from it. We have described this in terms of a thermal environment that represents stored kinetic energy in the vacuum and that is responsible for where the particle is being guided to. For example, consider particle propagation coming out from a Gaussian slit. For a particle exactly at the center of the Gaussian, the diffusive momentum contributions from the heated up environment will on average cancel each other for symmetry reasons. However, the further off the particle is from that center, the stronger the symmetry will be broken, thus resulting in a position-dependent net acceleration or deceleration, respectively – in effect, resulting in the decay of the wave packet. (For a detailed analysis, see [11].) In other words, due to wave-like diffusive propagations originating from the particle’s bounces to stir up the medium of the vacuum, particle paths can be influenced by the agitations of the vacuum even in places where no other particle is around.

As already mentioned, we have shown that the spreading of a wave packet can be exactly described by combining the forward (convective) with the orthogonal diffusive velocity fields. The latter fulfill the condition of being unbiased w.r.t. the convective velocities, i.e. the orthogonality relation for the *averaged* velocities derived in [11] is $\overline{\mathbf{v}\mathbf{u}} = 0$, since any fluctuations $\mathbf{u} = \delta(\nabla S/m)$ are shifts along the surfaces of action $S = \text{const}$. Moreover, the fluctuations can be directed towards the left or towards the right from the mean (i.e. from the Ehrenfest trajectory), which leads us to introduce the notations \mathbf{u}_{iL} and \mathbf{u}_{iR} , respectively.

Reducing the general case discussed in [12] to the double-slit case, one notes for the first and second channels the emergent velocity vectors $\mathbf{v}_{1(2)}$, $\mathbf{u}_{1(2)R}$, and $\mathbf{u}_{1(2)L}$, together with associated amplitudes $R_{1(2)}$, respectively. In order to completely accommodate the totality of the system of currents present, one obtains a local wave intensity for any velocity component, e.g. for \mathbf{v}_1 , by the pairwise projection on the unit vector $\hat{\mathbf{v}}_1$ weighted by R_1 of the totality of all amplitude weighted unit velocity vectors being operative at (\mathbf{x}, t) :

$$P(\mathbf{v}_1) = R_1 \hat{\mathbf{v}}_1 \cdot (\hat{\mathbf{v}}_1 R_1 + \hat{\mathbf{u}}_{1R} R_1 + \hat{\mathbf{u}}_{1L} R_1 + \hat{\mathbf{v}}_2 R_2 + \hat{\mathbf{u}}_{2R} R_2 + \hat{\mathbf{u}}_{2L} R_2). \quad (3)$$

The local current attributed to each velocity component is defined as the corresponding “local” intensity-weighted velocity, e.g. for \mathbf{v}_1 it is given as $\mathbf{J}(\mathbf{v}_1) = \mathbf{v}_1 P(\mathbf{v}_1) = \mathbf{v}_1 (R_1^2 + R_1 R_2 \cos \varphi)$. The local intensity of a partial current is dependent on all other currents, and the total current itself is composed of all partial components, thus constituting a representation of what we call *relational causality*. After a short calculation, the total current turns out as $\mathbf{J}_{\text{tot}} = \mathbf{v}_1 P(\mathbf{v}_1) + \mathbf{u}_{1R} P(\mathbf{u}_{1R}) + \mathbf{u}_{1L} P(\mathbf{u}_{1L}) + \mathbf{v}_2 P(\mathbf{v}_2) + \mathbf{u}_{2R} P(\mathbf{u}_{2R}) + \mathbf{u}_{2L} P(\mathbf{u}_{2L})$, which, by identifying the resulting diffusive velocities $\mathbf{u}_{iR} - \mathbf{u}_{iL}$ with the effective diffusive velocities \mathbf{u}_i for each channel, finally leads to

$$\mathbf{J}_{\text{tot}} = R_1^2 \mathbf{v}_1 + R_2^2 \mathbf{v}_2 + R_1 R_2 (\mathbf{v}_1 + \mathbf{v}_2) \cos \varphi + R_1 R_2 (\mathbf{u}_1 - \mathbf{u}_2) \sin \varphi. \quad (4)$$

The trajectories or streamlines, respectively, are given by

$$\dot{\mathbf{x}} = \mathbf{v}_{\text{tot}} = \frac{\mathbf{J}_{\text{tot}}}{P_{\text{tot}}}. \quad (5)$$

As first shown in [13], by re-inserting the expressions for convective and diffusive velocities, respectively, i.e.

$$\mathbf{v}_i = \frac{\nabla S_i}{m}, \quad \text{and} \quad \mathbf{u}_i = -\frac{\hbar}{m} \frac{\nabla R_i}{R_i}, \quad (6)$$

one immediately identifies Eq. (5) with the Bohmian guidance equation and Eq. (4) with the quantum mechanical pendant for the probability density current [14]. As we have shown also

the latter identity, we are assured that our results are the same as those of standard quantum mechanics – provided, of course, that generally (i.e. in the standard quantum as well as in our ansatz) the idealization of using Gaussians or similar regular distribution functions is applicable for the high degrees of attenuation studied here. However, as in our model we can also make use of the velocity field to plot the averaged particle trajectories, we can in principle provide a more detailed picture, in similar ways to the Bohmian one, but still not relying on any quantum mechanical tool like a wave function, for example.

In interpreting their results of the beam attenuation experiments with neutrons, Rauch *et al.* found evidence in support of the complementarity principle. That is, the more pronounced the visibility of the interference fringes, the less which-path knowledge one can have of the particle propagation, and *vice versa*: the higher the probability is for a particle to take a path through one certain slit, the less visible the interference pattern becomes. This was in fact confirmed in the above-mentioned neutron interferometry experiments, albeit to a lesser degree for very low counting rates. In particular, the authors of [4, 5] often use expressions such as the “particle-like” or the “wave-like” nature of the quantum system studied, depending on whether which-path information or interference effects are dominant, respectively. While this is all correct as far as the mentioned papers are concerned, an extrapolation of the use of “particle-like” or “wave-like” attributed to more extreme intensity hybrids is not guaranteed. In fact, we shall show below a particular effect which undermines said dichotomy of “particle-like” and “wave-like” features, thereby calling for an improved, more general analysis of possible relationships between particle and wave features.

2. The quantum sweeper effect during stochastic beam attenuation in the double slit and its superclassical modeling

Let us start with a discussion of stochastic attenuation using a coherent beam in a double-slit experiment. With the intensity distribution being recorded on a screen, we are going to discuss a particular effect of the attenuation of one of the two emerging Gaussians at very small transmission factors. With the appropriate filtering of the particles going through one of the two slits, the recorded probability density on a screen in the surroundings of the experiment will appear differently than what one would normally expect. That is, even if one had a low beam intensity coming from one slit, one would expect the following scenario according to the usual quantum mechanical heuristics: The interference pattern would more and more become asymmetric in the sense that the contributions from the fully open slit would become dominant until such a low counting rate from the attenuated slit is arrived at that essentially one would have a one-slit distribution of recorded particles on the screen.

Interestingly, this is not exactly what one obtains at least for very low values of a when going through the calculations and/or computer simulations with our superclassical bouncer model. The latter consists, among other features, in an explicit form of the velocity field emerging from the double slit, as well as of the probability density current associated with it.

Fig. 1 shows the *quantum sweeper effect*: a series of probability density distributions plus averaged trajectories for the case that the intensity in slit 2 is gradually diminished. We use the same model as in [13], or [15], respectively: particles (represented by plane waves in the forward y -direction) from a coherent source passing through “soft-edged” slits in a barrier (located along the x -axis) and recorded at a screen in the forward direction, i.e. parallel to the barrier. This situation is described by two Gaussians representing the totality of the effectively “heated-up” path excitation field, one for slit 1 and one for slit 2, whose centers have the same distances from the plane spanned by the source and the center of the barrier along the y -axis, respectively. Now, with ever lower values of the transmission factor a during beam attenuation, one can see a steadily growing tendency for the low counting rate particles of the attenuated beam to become swept aside. In our model, this is straightforward to understand, because we have the analytical

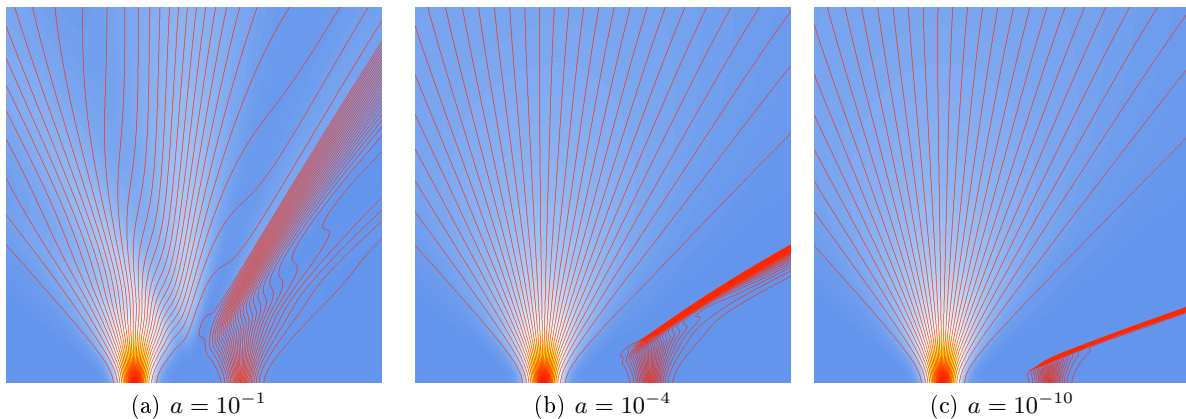


Figure 1: Trajectory behavior during the *quantum sweeper effect* for different transmission factors a at the right slit of a double slit setup: With ever lower values of a , one can see a steadily growing tendency for the originally dominant interference fringes to disappear and for the low counting rate particles of the attenuated beam to become swept aside. In our model, this phenomenology is explained by processes of diffusion due to the presence of accumulated kinetic energy mainly in the “strong” beam. The sweeper effect is thus the result of the vacuum heat sweeping aside the very low intensity beam, with a “no crossing” line defined by the balancing out of the osmotic momenta coming from the two beams, respectively. Throughout this paper, to demonstrate the effect more clearly, the same number of trajectories for each slit is displayed.

tools to differentiate between the forward propagations \mathbf{v}_i and the diffusive influences of velocities \mathbf{u}_i , as distinguishable contributions from the different slits i . Thus, it is processes of diffusion which are seen in operation here, due to the presence of accumulated heat (i.e. kinetic energy), primarily in the “strong” beam, as discussed in the previous Section. So, in effect, we understand Fig. 1 as the result of the vacuum heat sweeping aside the very low intensity beam, with a “no crossing” line defined by the balancing out of the diffusive momenta, $m(\mathbf{u}_1 + \mathbf{u}_2) = 0$.

Importantly, for certain slit configurations and sizes of the transmission factor, the sweeper effect leads to a bunching of trajectories which may become deflected into a direction almost orthogonal to the original forward direction. In other words, one would need much wider screens in the forward direction to register them, albeit then weakened due to a long traveling distance. On the other hand, if one installed a screen orthogonal to the “forward screen”, i.e. one that is parallel to the original forward motion (and thus to the y -axis), one could significantly improve the contrast and thus register the effect more clearly. Further, we note that changing the distance between the two slits does not alter the effect, but demonstrates the bunching of the low counting rate arrivals in essentially the same narrow spatial area even more drastically. So, again, if one places a screen not in the forward direction parallel to the barrier containing the double slit, but orthogonally to the latter, one registers an increased local density of particle arrivals in a narrow spatial area under an angle that is independent of the slit distance.

Let us now turn to the case of decoherent beams. For, although we shall refrain from constructing a concrete model of decoherence and implementing it in our scheme, we already have the tools of an effective theory, i.e. to describe decoherence without the need of a specified mechanism for it. Namely, as full decoherence between two (Gaussian or other) beams is characterized by the complete absence of the interference term in the overall probability distribution of the system, this means that $P_{\text{tot}} = R_1^2 + R_2^2$, since the interference term

$$R_1 R_2 (\mathbf{v}_1 + \mathbf{v}_2) \cos \varphi = 0. \quad (7)$$

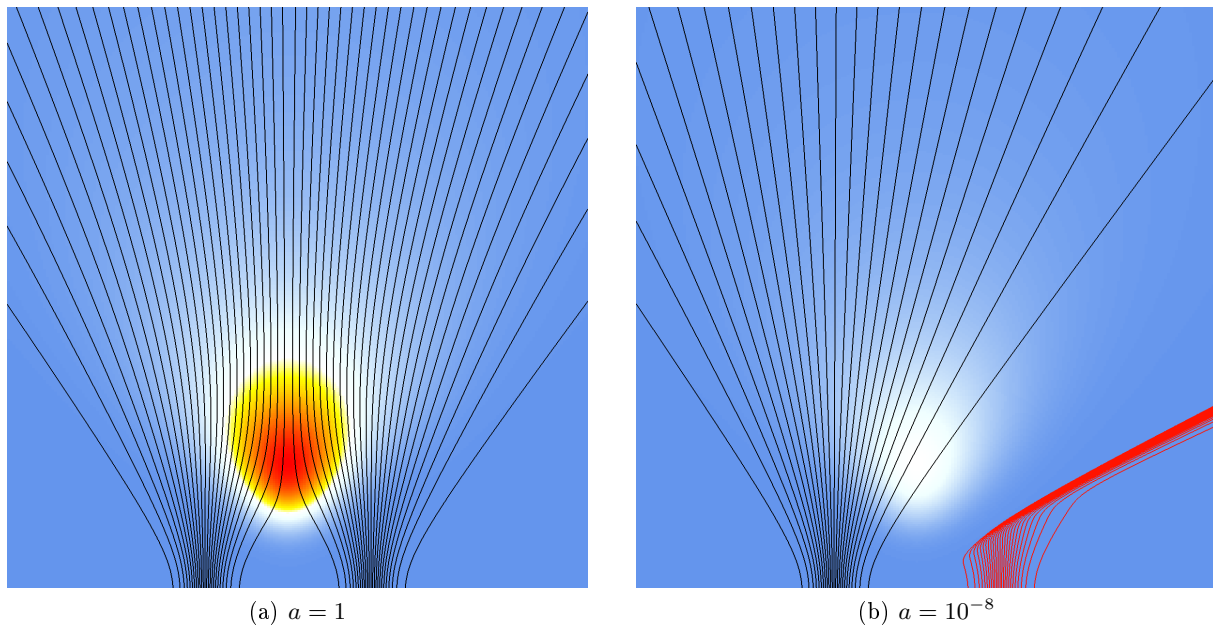


Figure 2: Double-slit experiment with completely incoherent channels. (a) The average trajectories never cross the central symmetry line, a fact due to the diffusion related “hot spot” indicated in red-to-yellow-to-white (depicting both interference terms of the total current (4)), which represents a kinetic energy reservoir that effectively gives particles a push in the forward direction. (b) The current’s interference term is now weakened by the factor $a = 10^{-8}$, which is why it does not affect the “strong” beam. However, it is sufficient for the attenuated beam to become deflected and thus to produce the sweeper effect.

If we therefore choose that on average one has $\cos \varphi = 0$, a situation with $\varphi = \frac{\pi}{2}$ effectively describes two incoherent beams in the double-slit system. What about the two interference terms in the probability density current (4), then? Well, the first term is identical with the vanishing (7), but the second term, with $\mathbf{u}_i = -\frac{\hbar}{m} \frac{\nabla R_i}{R_i}$ and $\varphi = \frac{\pi}{2}$ explicitly reads as

$$\frac{\hbar}{m} R_1 R_2 \left(\frac{\nabla R_2}{R_2} - \frac{\nabla R_1}{R_1} \right) = \frac{\hbar}{m} (R_1 \nabla R_2 - R_2 \nabla R_1). \quad (8)$$

As the distributions R_i may have long wiggly tails – summing up, after many identical runs, to a Gaussian with no cutoff, but spreading throughout the whole domain of the experimental setup [16] –, the expression (8) is not at all guaranteed to vanish. In fact, a look at Fig. 2 shows that there is an effect even for incoherent beams: Although the product $R_1 R_2$ is negligible and therefore leads to no interference fringes on the screen, nevertheless expression (8) has the effect of “bending” average trajectories so as to obey the “no crossing” rule well known from our model as well as from Bohmian theory.

In sum, then, performing a double-slit experiment with decoherent beams leads to an emergent behavior of particle propagation which can be explained by the effectiveness of diffusion waves with velocities u_i interacting with each other, thereby creating a “hot spot” where the intensity of the diffusive currents is highest and leads to a deflection into the forward direction such that no crossing of the average velocities beyond the symmetry line is made possible (Fig. 2a). This is therefore in clear contradiction to the scenario where only one slit is open for the particle to go through. If the slits are not open simultaneously, the particles could propagate to locations beyond the symmetry line, i.e. to locations forbidden in the case of the second slit being open [17].

As our velocity fields \mathbf{v}_i and \mathbf{u}_i (6) are identical with the Bohmian and the “osmotic” momentum, respectively, one can relate them also to the technique of weak measurements. The latter have turned out [18–20] to provide said velocities as “weak values”, which are just given by the real and complex parts of the quantum mechanical expression $\frac{\langle \mathbf{r} | \hat{p} | \Psi(t) \rangle}{\langle \mathbf{r} | \Psi(t) \rangle}$, i.e. the weak values associated with a weak measurement of the momentum operator \hat{p} followed by the usual (“strong”) measurement of the position operator \hat{r} whose outcome is \mathbf{r} . In other words, in principle the trajectories for intensity hybrids generally, and for the quantum sweeper in particular, are therefore accessible to experimental confirmation.

3. The quantum mechanical description of the sweeper effect

Let us now consider the stochastic attenuation discussed above in purely quantum mechanical terms. As already mentioned, the probability density distribution is given by Equation (2). A graphic representation of this distribution in a distance of 5m from the double slit is shown in Fig. 3. Two cases of the attenuation factor at one of the two slits of a double slit system are shown, i.e. $a = 10^{-4}$ and $a = 10^{-8}$ affecting the right slit, respectively. As is to be expected, on a linear scale the distribution will appear as if practically the whole intensity goes through the left un-attenuated slit (Fig. 3a). Zooming in with a factor of 1,000 as shown in Fig. 3b, one can see the faint rest of interference phenomena for the case of $a = 10^{-4}$ (blue), whereas for $a = 10^{-8}$ (red) apparently smooth behavior is seen. Still, the full effect is best visible on the logarithmic scale shown in Fig. 3c. Compared to the dotted initial distributions for the cases of $a = 10^{-4}$ (blue) and $a = 10^{-8}$ (red), respectively, the whole distribution clearly shows interference phenomena which have been “swept aside” far to the right. Thus, the quantum sweeper effect is confirmed also via orthodox language.

The bunching together of low counting rate particles within a very narrow spatial domain, or channel, respectively, counters naive expectations that with ever higher beam attenuation nothing interesting may be seen any more. The reason why these expectations are not met is given by the explicit appearance of the nonlinear structure of the probability density current (4) in these domains for very low values of a .

4. Summary and implications

As for implications of our finding presented here, we shall now briefly remark on its relevance with respect to the issue of wave-particle duality. Considering the appearance of compressed interference fringes in the attenuated beam in Fig. 1, it is indisputable that one has to do with the result of a wave-like behavior. This is confirmed in Fig. 2b where the decoherent scenario is characterized by the complete absence of such wave-like behavior like interference fringes. This means, however, that an often used argument to describe the complementarity between wave- and particle-like behavior in the double slit experiment, or in interferometry, respectively, has only limited applicability, as it does not apply to intensity hybrids, since in our model the wave-like contributions due to diffusion are always present. Specifically, the relation for pure states [21]

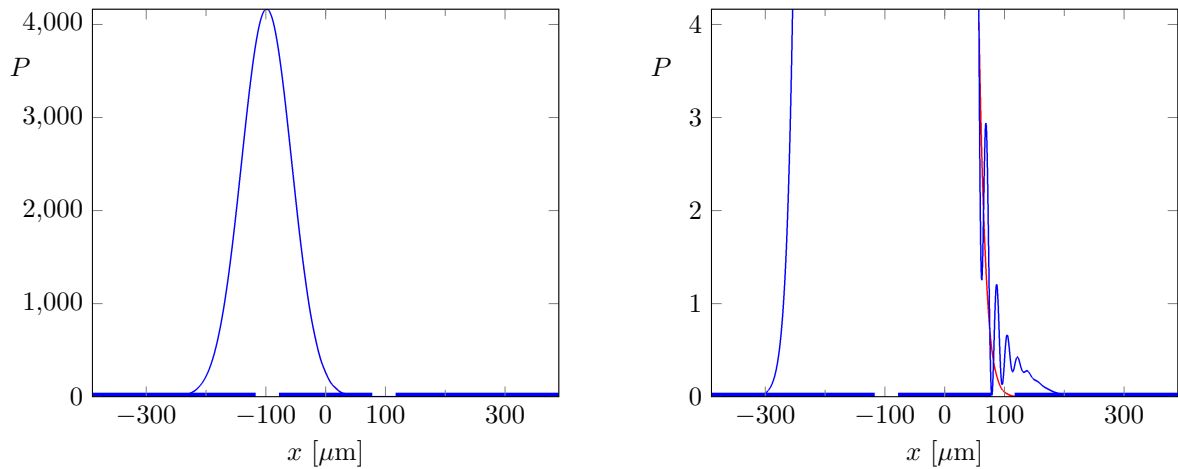
$$D^2 + V^2 = 1, \quad (9)$$

with distinguishability

$$D = \left| \frac{R_1^2 - R_2^2}{R_1^2 + R_2^2} \right| \quad (10)$$

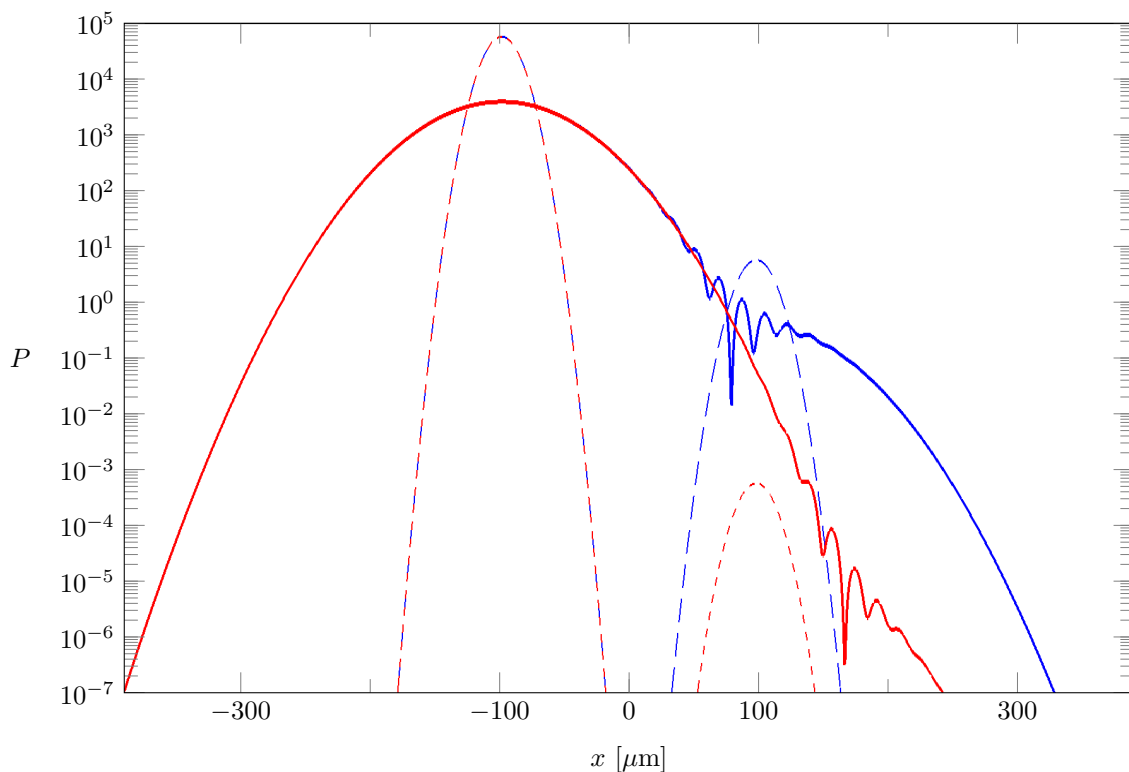
representing the particle-related which-path information and visibility

$$V = \frac{|R_1 + R_2|^2 - |R_1 - R_2|^2}{|R_1 + R_2|^2 + |R_1 - R_2|^2} = \frac{2R_1R_2}{R_1^2 + R_2^2} \quad (11)$$



(a) Probability density distribution P in a distance of 5 m from the double slit. The two cases of the attenuation factor at the right slit of a double slit system, i.e. $a = 10^{-4}$ and $a = 10^{-8}$, respectively, essentially provide the same distribution at moderate resolution.

(b) Same as in (a), but zooming in with a factor of 1,000. Now the two cases are discernible: note the faint rest of interference phenomena for the case of $a = 10^{-4}$ (blue), whereas for $a = 10^{-8}$ (red) apparently smooth behavior is seen.



(c) Same as in (a), but now on a logarithmic scale. Dotted initial distributions for the cases of $a = 10^{-4}$ (blue) and $a = 10^{-8}$ (red), respectively, develop into distributions clearly showing interference phenomena which have been “swept aside” far to the right. This sweeper effect is due to the explicit appearance of the nonlinear structure of the probability density current in these domains for very low values of a .

Figure 3: The sweeper effect as described by quantum mechanics

the contrast of the interference fringes in the standard quantum mechanical double slit scenario, suggests that with ever lower values of a ever lower values of V are implied in a constantly decreasing manner. In our case, by considering the superclassical nature of the sweeper effect, we find a deviating, characteristic signature at very low values of $a \lesssim 10^{-4}$. In this domain, the usual expectation would be that practically one has arrived at the “particle” side of the complementarity principle, i.e. essentially a one-slit distribution, with wave-like phenomena having almost disappeared. However, if one has a very strongly attenuated beam, the emerging behavior of its outgoing trajectories is different from a one-slit particle distribution scenario if the other slit is open and un-attenuated. The increased local relative contrast corresponding to a bunching of trajectories and due to said nonlinear effect of the probability density current is to be captured by a vertical screen (i.e. parallel to the y -axis) for optimal visibility.

We have thus shown that for transmission factors below $a \lesssim 10^{-4}$ in intensity hybrids, new effects appear which are not taken into account in a naive, i.e. linear, extrapolation of expectations based on higher-valued transmission factors. We have described the phenomenology of these *quantum sweeper* effects, including the bunching together of low counting rate particles within a very narrow spatial domain, or channel, respectively. However, we also stress that these results are in accordance with standard quantum mechanics, since we just used a re-labeling and re-drawing of the constituent parts of the usual quantum mechanical probability density currents. However, concerning the explicit phenomenological appearances due to the nonlinear structure of the probability density current in the respective domains for very low values of a , our subquantum model is better equipped to deal with these appearances explicitly.

With the discovery of the quantum sweeper effect on the basis of a superclassical causal approach to quantum mechanics, we claim to have presented a first example as it was demanded by Rabi. We are optimistic that through further developments, both in superclassical theory employing subquantum mechanics and in weak measurement techniques capable of probing the latter regime, more unexpected new effects can be predicted and eventually be confirmed in experiment.

Acknowledgments

We thank Jan Walleczek for many enlightening discussions and the Fetzer Franklin Fund for partial support of the current work.

References

- [1] Freire Jr. O 2005 Science and exile: David Bohm, the cold war, and a new interpretation of quantum mechanics *HSPS* **36** 1–34, [arXiv:physics/0508184](#) [[physics.hist-ph](#)]
- [2] Grössing G, Fussy S, Mesa Pascasio J and Schwabl H 2015 Extreme beam attenuation in double-slit experiments: Quantum and subquantum scenarios *Ann. Phys.* **353** 271–281, [arXiv:1406.1346](#) [[quant-ph](#)]
- [3] Grössing G, Fussy S, Mesa Pascasio J and Schwabl H 2015 Implications of a deeper level explanation of the deBroglie–Bohm version of quantum mechanics *Quantum Stud.: Math. Found.* , [arXiv:1412.8349](#) [[quant-ph](#)] in press
- [4] Rauch H and Summhammer J 1984 Static versus time-dependent absorption in neutron interferometry *Phys. Lett. A* **104** 44–46
- [5] Rauch H, Summhammer J, Zawisky M and Jericha E 1990 Low-contrast and low-counting-rate measurements in neutron interferometry *Phys. Rev. A* **42** 3726–3732
- [6] Grössing G ed 2012 *Emergent Quantum Mechanics 2011* No. 361/1 (Bristol: IOP Publishing) Url: <http://iopscience.iop.org/1742-6596/361/1>
- [7] Grössing G, Elze H-T, Mesa Pascasio J and Walleczek J ed 2014 *Emergent Quantum Mechanics 2013* No. 504/1 (Bristol: IOP Publishing) Url: <http://iopscience.iop.org/1742-6596/504/1>
- [8] Fort E, Eddi A, Boudaoud A, Moukhtar J and Couder Y 2010 Path-memory induced quantization of classical orbits *PNAS* **107** 17515–17520
- [9] Couder Y and Fort E 2006 Single-particle diffraction and interference at a macroscopic scale *Phys. Rev. Lett.* **97** 154101

- [10] Couder Y and Fort E 2012 Probabilities and trajectories in a classical wave-particle duality *J. Phys.: Conf. Ser.* **361** 012001
- [11] Grössing G, Fussy S, Mesa Pascasio J and Schwabl H 2010 Emergence and collapse of quantum mechanical superposition: Orthogonality of reversible dynamics and irreversible diffusion *Physica A* **389** 4473–4484, [arXiv:1004.4596 \[quant-ph\]](#)
- [12] Fussy S, Mesa Pascasio J, Schwabl H and Grössing G 2014 Born's rule as signature of a superclassical current algebra *Ann. Phys.* **343** 200–214 [arXiv:1308.5924 \[quant-ph\]](#)
- [13] Grössing G, Fussy S, Mesa Pascasio J and Schwabl H 2012 An explanation of interference effects in the double slit experiment: Classical trajectories plus ballistic diffusion caused by zero-point fluctuations *Ann. Phys.* **327** 421–437, [arXiv:1106.5994 \[quant-ph\]](#)
- [14] Sanz A S and Miret-Artés S 2008 A trajectory-based understanding of quantum interference *J. Phys. A: Math. Gen.* **41** 435303, [arXiv:0806.2105 \[quant-ph\]](#)
- [15] Holland P R 1993 *The Quantum Theory of Motion* (Cambridge, UK: Cambridge Univ. Press)
- [16] Grössing G, Fussy S, Mesa Pascasio J and Schwabl H 2013 'Systemic nonlocality' from changing constraints on sub-quantum kinematics *J. Phys.: Conf. Ser.* **442** 012012, [arXiv:1303.2867 \[quant-ph\]](#)
- [17] Sanz A S and Borondo F 2009 Contextuality, decoherence and quantum trajectories *Chem. Phys. Lett.* **478** 301–306, [arXiv:0803.2581 \[quant-ph\]](#)
- [18] Leavens C R 2005 Weak measurements from the point of view of Bohmian mechanics *Found. Phys.* **35** 469
- [19] Wiseman H M 2007 Grounding Bohmian mechanics in weak values and bayesianism *New J. Phys.* **9** 165–176, [arXiv:0706.2522 \[quant-ph\]](#)
- [20] Hiley B J 2012 Weak values: Approach through the Clifford and Moyal algebras *J. Phys.: Conf. Ser.* **361** 012014, [arXiv:1111.6536v1 \[quant-ph\]](#)
- [21] Greenberger D M and Yasin A 1988 Simultaneous wave and particle knowledge in a neutron interferometer *Phys. Lett. A* **128** 391–394